A CONCEPT FOR A NOVEL POLYMER EXTRUDER.
PART II: ROTATIONAL BARREL SEGMENT

Hubert Dębski[1*], Bolesław Kiszka[2], António Gaspar-Cunha[3]

[1] Faculty of Mechanical Engineering, Department of Machine Design and Mechatronics, Lublin University of Technology, Nadbystrzycka 36, 20-618 Lublin, Poland; e-mail: h.debski@pollub.pl
[2] ZAMAK Mercator Sp. z o.o., . ul. J. Piłsudskiego 63, 32-050 Skawina, Poland; e-mail boguslawk@zamakmercator.pl
[3] Department Polymer Engineering, Institute Polymers & Composites, P-4800058 Guimaraes, University of Minho, Minho, Portugal; e-mail: agc@dep.uminho.pt
[*] Correspondence: h.debski@pollub.pl, Nadbystrzycka 36, 20-618 Lublin, Poland

Key Words: *finite element method, rotational barrel segment, polymer extruder, granulates.*

Abstract

This paper presents a novel concept of an extrusion machine for polymer plastics, polymer-matrix materials, and food processing applications. The design of the extruder includes a rotational barrel segment to enable kinematic activation in the process of plasticizing the material and improvement in the homogenization level. The tests included a FEM-based numerical analysis of the rotational barrel segment design. The numerical calculations comprised a fully coupled thermal-stress analysis, used to solve a non-linear geometric and physical problem. The numerical calculation results proved that the designed structural parts of the rotational barrel segment had sufficient strength and that the design of the rotational barrel segment was suitable in terms of the required temperature distribution within the structural parts. The numerical calculation tool used in the analysis was ABAQUS®, commercially available software.

1. Introduction

The methods used to process plastic materials are still being improved, with novel types and versions continuing to emerge, with plastic materials that can be created as mixtures of different plastics and new fillers produced from renewable sources [1] and nano-fillers [2]. Biodegradable and compostable plastics have been claiming an increasing market share. These products are made primarily using starch from wheat, corn or potatoes, or by supplementing plastics with various degradation accelerants [3, 4]. Most plastics of this type are not easily processed by standard extrusion or injection moulding. Processing based on standard plasticizing systems (primarily extruders) is becoming inefficient, unstable and costly. To ensure maximum processing efficiency, a plasticizing system must be optimised to the grain size and shape of the granulated materials [5], while the feed opening requires an optimised geometry and position relative to the centreline of the plasticizing screw [6]. A modification to the design characteristics of the grooved zone and its adaptation to the grain size and shape of the granulated material during the extrusion of plastic can be achieved by applying an active grooved zone in the extruder [7, 8]. However, an active grooved zone has little effect on the homogenisation of the plastic material in the plasticizing system. One novel method for mixing the plastic material in a plasticizing system is the application of a rotational barrel segment within the material feed zone [9]. E. Sasimowski presented the first study into the application of a rotational barrel segment in an extruder, identifying the optimum location of the segment [10] and evaluating the application effects during extrusion of LDPE [11]. The study did not include any adaptation of the screw design to the modified geometry of the plasticizing barrel, and used a standard screw mated with a geometrically non-uniform inner barrel surface, which featured a standard grooving pattern. Efforts were made to modify the design characteristics of the barrel inner surface to enable a suitable modification of the plasticizing screw design.

Innovative plasticizing systems have been developed for a single-screw extruder, complete with a rotational barrel segment, but varying in the geometrically non-uniform inner surface. However, before commercialising the developed solutions, a design optimisation process is required, which involves virtual modelling with an analysis of the kinematic performance parameters. The analysis is intended to eliminate potential points of collision between the moving parts of the plasticizing system. The design optimisation process is followed by a FEM numerical simulation which enables a thermal and strength assessment of the proposed design solution and specification of the most optimum versions, without the need for costly and lengthy testing. The tool used for this purpose will be the still improved ABAQUS®.

This paper presents a novel concept for an extruder plasticizing system which features an innovative rotational barrel segment that allows modification of the plasticizing screw geometry. The concept is fully functional, strength and thermal-tested, and ready for further stages towards commercialisation.

2. Concept for the extruder's rotational barrel segment

The initial design of the visualisation presented here was:
- A fully functional 3D model of the concept developed in SolidWorks. The model was tested for truth and collision. A virtual prototype was built to help determine if any potential irregularities would occur during the simulated movement.
- Certain design details were omitted (fasteners etc.), which were insignificant to the functional performance.

The design assumptions for the rotational barrel segment were:
- rotational barrel segment length of 1-4D, or 25 to 100 mm,
- barrel inner diameter 25 mm,
- maximum temperature resistance approx. 300°C,
- maximum operating pressure 200 bar,
- heated rotational barrel segment,
- rotational barrel segment rotatable, either in or opposite to the screw rotation direction,
- maximum rotational speed of the rotational barrel segment 150 rpm,
- coil flight profile on the barrel segment inner surface identical to the screw coil,
- sealed joints within the plasticizing system.

The concept model was completely novel, and represented as a CAD model. Heating of the rotational barrel segment was achieved by a system of heating straps. The heating straps were designed to be attached to sliding bushings made from a heat-resistant material. The heating straps were secured against rotation, with the fasteners attached to the heat insulators. The individual segments of the extruder barrel were designed to be clamped together with threaded bars, fitted with springs and nuts. This solution provided a constant clamping force, irrespective of the barrel temperature or linear expansion of the barrel components. The whole plasticizing system assembly, comprised of several barrel segments, were attached to a baseplate. The rotational barrel segment was located within the material feed area. The presented concept has innovative value and was filed for patent protection.

The concept of the rotational barrel segment is illustrated in Fig. 1. The concept applies to a plasticizing system based on a screw without a coil flight or with slight surface irregularities, both along the interface between the screw and the rotational barrel section. The rotational barrel segment inner surface featured a flight of coils identical to the flight on the screw.
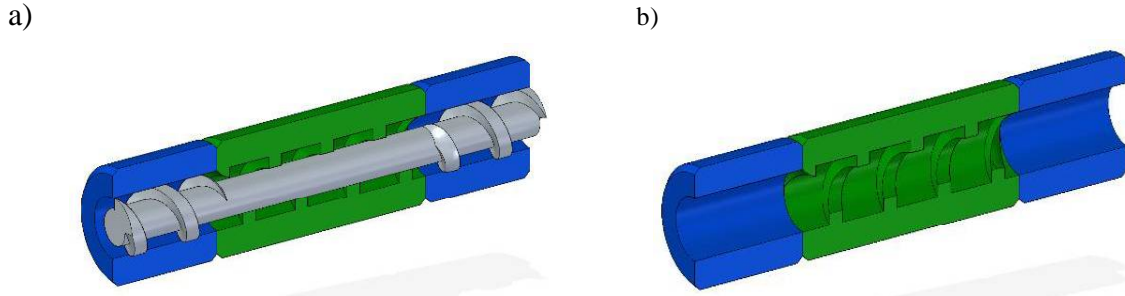
Fig. 1. Longitudinal section of the plasticizing system with a rotational barrel segment and a) a screw without a coil flight along the rotational barrel segment length, and b) without a screw

Considering the performance of the plasticizing system and the homogenization level of the extruded plastic material, the rotational barrel segment could rotate at a controlled, adjustable speed in the same direction of rotation as the screw, or the opposite direction. The difference between the rotational speed of the rotational barrel segment and the screw determined the blending ratio of the plastic material and the plasticizing system performance.

The design of a plasticizing system of this type poses some engineering challenges. One of the most significant of these is to ensure the required seal performance at the interface between the rotational barrel segment and the immovable segments of the extruder barrel. It would be optimum to use a seal made from a material with a thermal expansion coefficient higher than the material of the rotating components. This should ensure a full seal at varying temperatures. An important performance feature of the seal is the coefficient of friction, which should be low enough to ensure the lowest rate of tribological wear.

Given the complex structure of the rotational barrel segment, the inner surface of which featured a flight, it was necessary to include a split screw comprising two or more parts, connected with threaded fasteners. This should simplify the installation procedure of the screw and the rotating components.

3. Numerical analysis of the design

The numerical calculations involved a fully coupled thermal-stress analysis, including the interactions of the thermal and mechanical dependencies. The numerical calculations included the structural components of the rotational barrel segment of the extruder, designated as the 'extruder hot zone'. The objective of the numerical calculations was to determine the temperature distribution during continuous operation of the extruder and determine the stress intensity of the rotational barrel segment structural components by determination of the reduced stress distribution. The numerical calculations solved a non-linear geometric and physical problem, formulated as follows [8]:

$$\begin{bmatrix} K_{uu} & K_{u\theta} \\ K_{\theta u} & K_{\theta\theta} \end{bmatrix} \begin{Bmatrix} \Delta_u \\ \Delta_\theta \end{Bmatrix} = \begin{Bmatrix} R_u \\ R_\theta \end{Bmatrix}, \tag{1}$$

where Δ_u and Δ_θ are the respective corrections to the incremental displacement and temperature, K_{ij} are the submatrices of the fully coupled Jacobian matrix, while R_u and R_θ are the mechanical and thermal residual vectors, respectively. The equation was solved with an incremental-iterative Newton Raphson method and a non-symmetric matrix [13-17].

The process of digitizing the concept structure was performed with type C3D4T solid elements. The finite element type selected featured 4 nodes, 3 translational degrees of freedom per node, and one additional degree of freedom to permit a definition of the temperature problem. The finite element was a tetragon and defined by a 1st order form function with full integration. The

numerical model of the rotational barrel segment is illustrated in Fig. 2a. The boundary conditions of the digital model were defined by locking the translational degrees of freedom, X, Y and Z, and the respective boundaries of the segment, see Fig. 2b.

The numerical model included mechanical and thermal loads, analysed in three steps. The mechanical load analysed in the two first steps of the numerical calculations was a centrifugal load generated by the rotation of the barrel segment at n = 150 rpm (Fig. 3a) and the pressure load of the rotational barrel segment inner surface from the pressure generated by the plastic material within, p = 50 MPa, constant across the whole inner surface (Fig. 3b).
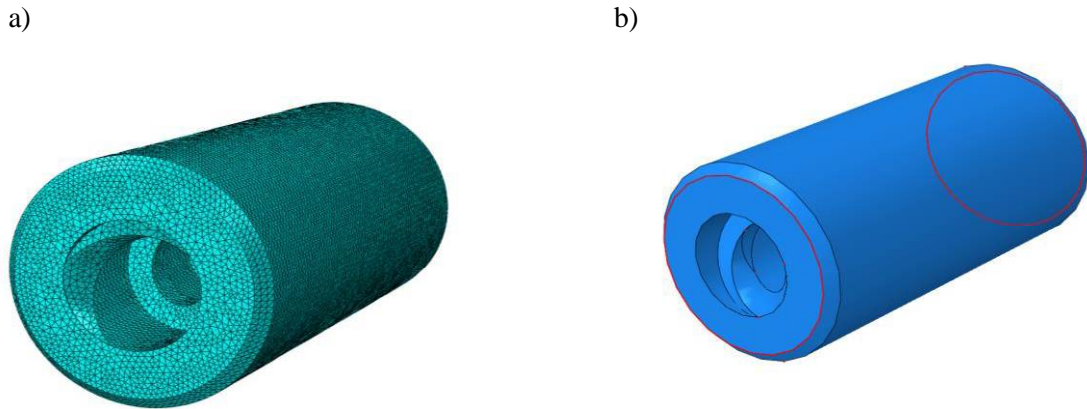
a)   b)

Fig. 2. FEM model of the rotational barrel segment: a) finite element mesh, b) areas with defined boundary conditions

a)   b)
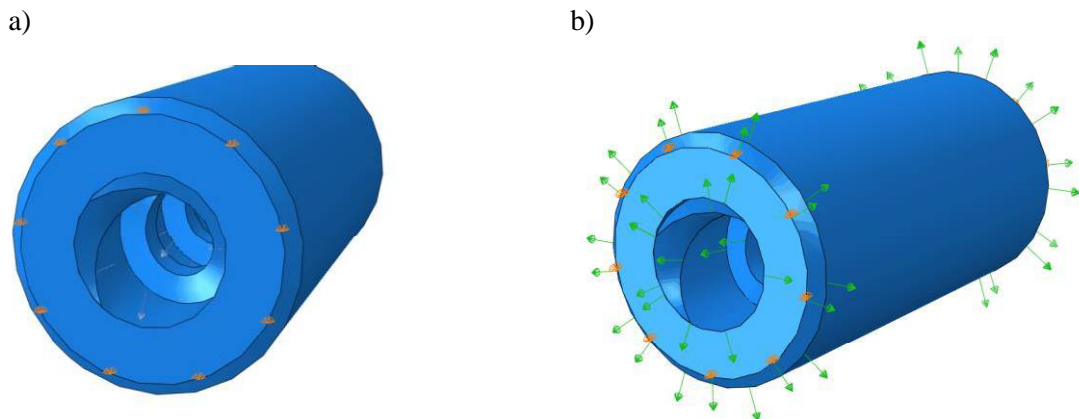

Fig. 3. Mechanical load of the rotational barrel segment: a) centrifugal load from the rotation of the segment, b) pressure load from the transported plastic material

The third step of the numerical analysis involved the coupled thermal-stress calculations. In this step of the numerical calculations, the initial conditions assumed was the state of the strain and stress of the model due to the mechanical loads, while the initial temperature of the model was T_0 = 22°C. The thermal load of the model was represented by temperature T = 150°C, generated by the friction of the plastic material transported by the screw and transmitted to the inner surface of the rotational barrel segment. An additional thermal load was used, the temperature generated by the heating of the rotational barrel segment outer surface, T = 150°C, see Fig. 4.

The modelled material assumed for the rotational barrel segment was 40HM steel. For this steel, the numerical calculations had a bi-linear material model defined with an elastic-plastic response; the material properties are listed in Table 1.
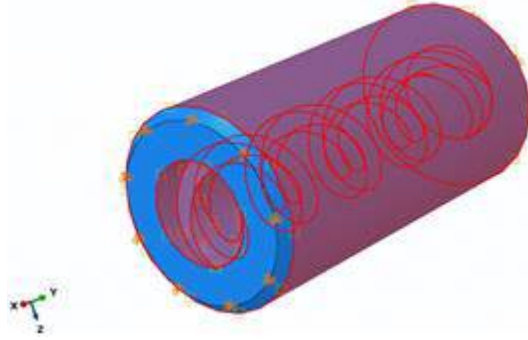
Fig. 4. Thermal load of the rotational barrel segment model

Table 1. Mechanical and thermal properties of 40HM steel

Young's modulus E [Pa]	Poisson's ratio [-]	Yield strength R_e [Pa]	Tensile strength R_m [Pa]	Elongation at break [%]	Density ρ [kg/m³]	Coefficient of linear expansion [-]	Thermal conductivity coefficient λ [W/(m·K)]	Specific heat [J/(kg·K)]
2.1e+11	0.3	8.8e+11	1.03e+12	10	7860	1.2e-5	58	450

4. Numerical calculation results

The numerical calculations for the rotational barrel segment structure exposed to mechanical and thermal loads were limited to static calculations of a non-linear geometric and physical problem. The non-linear system of equations was solved by application of an incremental-iterative Newton Raphson method. The strength analysis of the rotational barrel segment was based on the distributions of the reduced stress, which was determined with the Huber-Mises-Hencky (HMH) strength theory. The maps of HMH stresses are illustrated in Fig. 5.
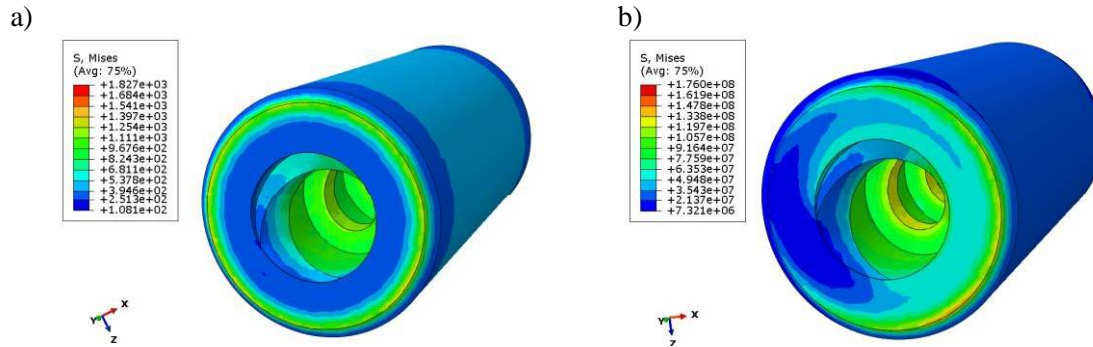
a)

b)

Fig. 5. Maps of reduced HMH stress in the rotational barrel segment model:
a) centrifugal force load, b) centrifugal force and internal pressure load

The reduced HMH stress maps for the structural mechanical stress allowed the determination of stress intensity of the material assumed for the rotational barrel segment. Fig. 5a shows that the reduced stresses generated by the rotation of the barrel segment at n = 150 rpm caused no stress in the segment, which reached a maximum of $\sigma_z \approx 0.0018$ MPa. When complemented by the internal pressure of p = 50 MPa in the rotating segment (Fig. 5b) the stress level reached $\sigma_z \approx 176$ MPa.

The next stage of the numerical calculations was a fully coupled thermal-stress analysis, the results of which allowed the determination of the temperature distribution in the material of the rotational barrel segment and the reduced HMH stresses generated by the thermal load. The results

represented the condition of continuous operation of the extruder for a duration of 18,000 s (5 h). The calculation results are illustrated in Fig. 6. The thermal calculations showed that the structure reached steady state conditions.

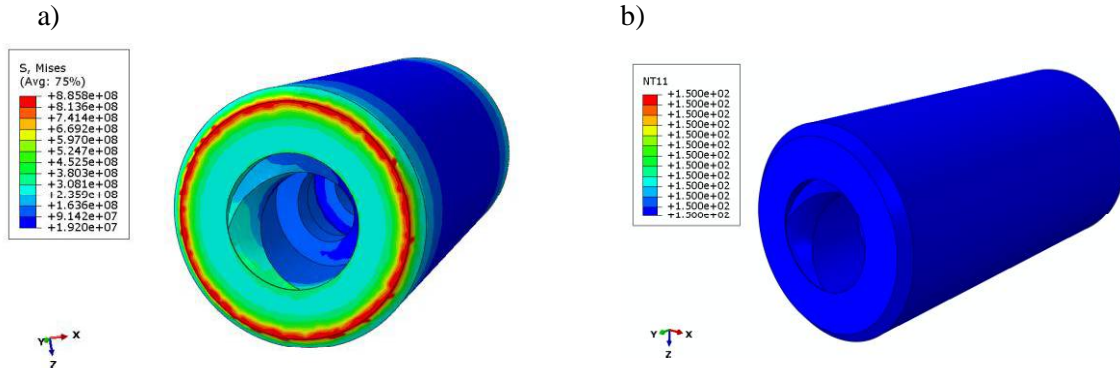a)   b)

Fig. 6. Results of the fully coupled thermal-stress analysis: a) temperature distribution within the rotational barrel segment, b) distribution of the reduced HMH stress

The steady state was achieved when the temperature in the whole rotational barrel segment remained at T = 150°C. The temperature corresponded to the temperature of the thermal load applied from outside and inside the structure. The thermal load caused a significant increase in the reduced HMH stresses, the total of which was the sum of the mechanical and thermal loads, at $\sigma_z \approx$ 885 MPa. The resulting stress value was slightly above the yield point of 40HM steel, at R_e = 880 MPa according to the assumed material properties. However, it can be seen (Fig. 6b) that the highest stresses were generated at the edges where the restraint of the model was defined. This caused a locally elevated stress intensity in the model.

Given the above, it can be stated that the designed structure of the rotational barrel segment had sufficient strength to prevent any compromise of the extruder operating safety.

5. Computer simulations

The computer simulations were demonstrated using three cases, with examples of the calculations of the plastic extrusion process based on a plasticizing system with a rotational barrel section.

In this case (case1) the length of the rotational barrel (L_b) is 1D. As can be seen in Table 2, eight screw speeds of the RBS (N_b) were teste. First, it was considered a situation where this speed is nil. The Table 2 presents the different values necessary to analyse the performance of the RBS. The most important aim been to maximize the mixing, quantified here by WATS, while little changes must be obtained in the remaining criteria, i.e., output, melt temperature at die exist (T_{melt}), mechanical power consumption (Power), length of screw required for melting ($L_{melting}$) and viscous dissipation.

Table 2. Influence of Rotational Barrel Segment ($L_b = 1D$: $L/D \in [16; 17]$)

N_b (rpm)	Output (kg/hr)	T_{melt} (°C)	Power (W)	$L_{melting}$ (m)	WATS	Viscous Dissipation
0.0	5.3	188.9	2278	14.6	308.0	1.46
-20.0	5.4	189.0	2295	14.8	334.2	1.46
-40.0	5.5	189.2	2331	14.8	328.4	1.46
-80.0	5.5	189.3	2383	14.8	317.3	1.46
-120.0	5.7	189.8	2397	15.1	307.9	1.44
20.0	5.3	188.8	2283	14.3	339.2	1.47
40.0	5.2	188.8	2238	14.4	347.5	1.47
80.0	4.9	188.8	2214	14.2	358.0	1.48
120.0	4.9	189.0	2185	14.0	366.0	1.48

A negative Rotational Barrel Segment (RBS) speed means that the RBS rotates in the opposite direction to the screw. Since the screw speed was fixed at 120 rpm, an RBS speed of -120 rpm gave the largest differences in mixing degree (WATS), while the other characteristics showed no significant changes, except the output, which decreased (Table 2). When the pressure profiles are considered (Fig. 7), it can be seen that the high WAT performance occurred when the pressure decreased, which influenced the output undesirably.
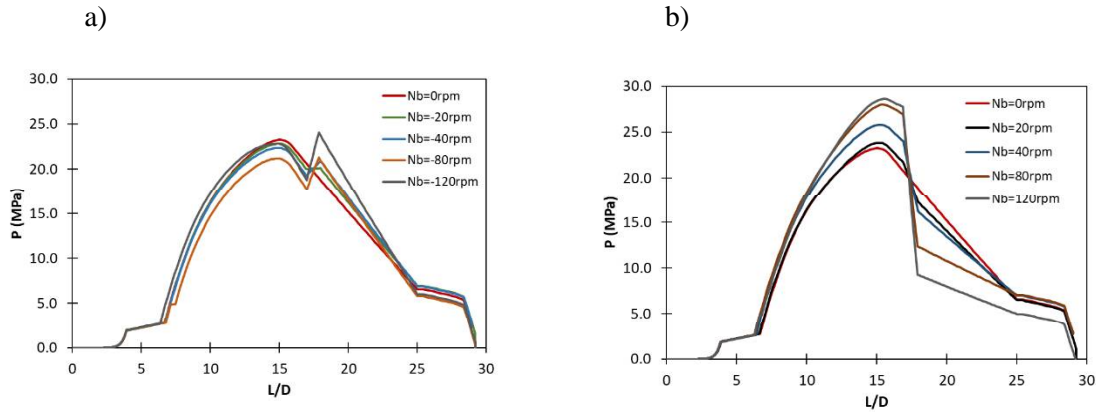
a)   b)

Fig. 7. Pressure profile for case 1 with RBS rotation: a) in the opposite direction to the screw, b) in the same direction as the screw

Table 3 and Figure 8 (case 2) present the same type of results as those for case 1, but now considering the length of the RBS equal to 3D. The conclusions are the similar to case 1. However, in this case, it is important to note that the best mixing performance was obtained when the pressure decreased below zero, with Nb equal to 80 and 120 rpm (Fig. 8b). In practice this cannot occur, which is an advantage of analysing the different geometries and operating conditions using computer programs.

Taking this into account, one potential solution is to increase the pressure before the extruder to overcome this limitation in pressure. This can be achieved by using a barrel with grooves in the solids conveying zone. See case 3 below.

Table 3. Influence of Rotational Barrel Segment ($L_b = 3D$: $L/D \in [16; 19]$)

N_b (rpm)	Output (kg/hr)	T_{melt} (°C)	Power (W)	$L_{melting}$ (m)	WATS	Viscous Dissipation
0.0	5.3	188.9	2278	14.6	308.0	1.46
-20.0	5.5	189.3	2358	14.8	383.3	1.46
-40.0	5.8	190.1	2395	15.5	376.4	1.45
-80.0	6.1	191.1	2583	15.6	339.9	1.44
-120.0	6.4	192.2	2834	15.8	315.6	1.43
20.0	5.1	188.5	2241	14.1	405.1	1.47
40.0	4.8	188.2	2163	14.0	422.9	1.48
80.0	4.0	187.7	2195	12.8	451.0	1.50
120.0	3.7	187.8	2100	12.2	484.1	1.51

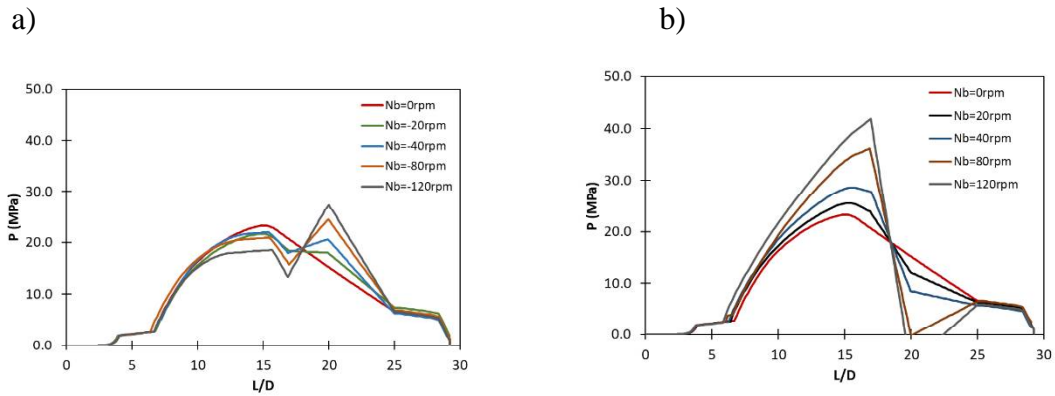a)   b)

Fig. 8. Pressure profile for case 2 with RBS rotation a) in the opposite direction to the screw, b) in the same direction as the screw

By analysis of Table 4 and Figure 9 (case 3), it can be seen that the addition of grooves in the solids conveying zone helps resolve the zero-pressure issue under some conditions, such as at an RBS speed of 80 rpm. This allows good mixing behaviour to be achieved. However, in all cases, a balance must be made between the mixing and the output.

Table 4. Influence of Rotational Barrel Segment (L_b = 3D: $L/D \in$ [16; 19]; with grooves)

N_b (rpm)	Output (kg/hr)	T_{melt} (°C)	Power (W)	$L_{melting}$ (m)	WATS	Viscous Dissipation
0.0	5.3	188.9	2278	14.6	308.0	1.46
-20.0	5.7	188.4	2975	14.4	372.1	1.13
-40.0	5.8	188.9	3077	14.6	358.0	1.11
-80.0	6.1	189.7	3306	15.0	330.2	1.12
-120.0	6.4	191.1	3488	15.0	304.6	1.13
20.0	5.3	187.7	2798	14.0	398.4	1.10
40.0	5.0	187.6	2714	13.6	411.6	1.21
80.0	4.3	187.6	2767	11.7	430.0	1.30
120.0	3.9	188.0	2771	6.1	482.4	1.28

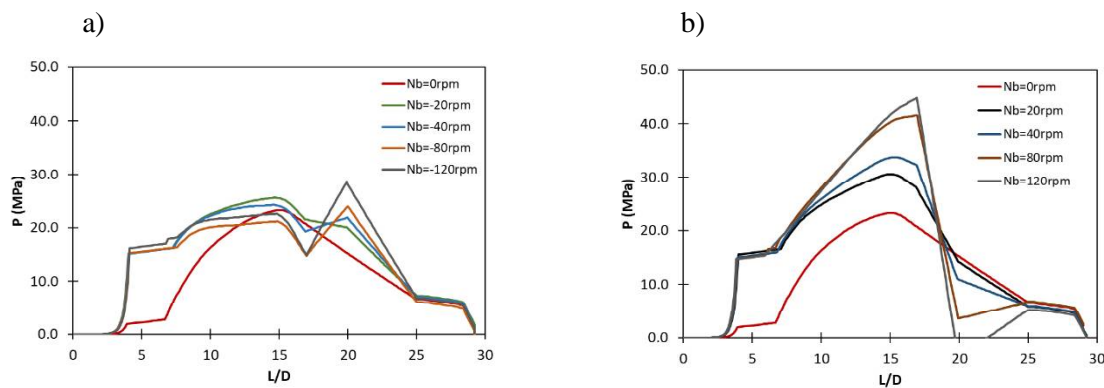a)   b)

Fig. 9. Pressure profile for case 3 with RBS rotation a) in the opposite direction to the screw, b) in the same direction as the screw

6. Conclusions

This paper presents a novel concept of a rotational barrel segment for an extruder used for plastic materials, where the inner surface of the segment featured a screw geometry engaged with a smooth plasticizing screw zone. This solution could help improve the efficiency of handling granulated LDPE through the plasticizing system of an extruder, with the LDPE plasticized within

the hot zone. The work discussed included a FEM numerical analysis, which enabled a strength analysis of the rotational barrel segment.

The calculations described a complex problem using a fully coupled thermal-stress analysis. The solution to the problem allowed determination of the temperature distribution within the material of the rotational barrel segment and determination of the reduced HMH stress values caused by the mechanical load (from the rotation of the segment and the pressure from the transported plastic material in the segment) and thermal load (from the friction of the granulated LDPE handled through the plasticizing system and the heating of the segment's outer surface). The results demonstrated that the predominant stress of the rotational barrel segment was thermal and present for continuous operation of the extruder over an 18,000 s period, causing a significant increase in the reduced stress levels close to the yield point of the material of the rotational barrel segment. An evaluation of the results allows the conclusion that the maximum stress values achieved were an effect of the boundary conditions applied in the concept model; hence the stress levels did not compromise the operating safety of the extruder. The resulting temperature distributions demonstrated that continuous operation of the extruder reached a steady state condition, as defined by the steady temperature throughout the volume of the material of the rotational barrel segment and equal to the temperature of the thermal load of the outer and inner surface of the segment.

The conclusion that can drawn in this computational study, in which the influence of the length and the velocity of the RBS were assessed, is related with the balance between the output of the extruder and the mixing degree that can be accomplished by the RBS, but taking into consideration, simultaneously, the pressure profile along the extruder. The better balance is can be obtained when a barrel section with grooves is used in the solids conveying zone.

The proposed concept is a novel solution for a plastic extruder, which has entered a commercialisation process, with the fabrication and implementation stages almost fully completed.

REFERENCES

[1] Głogowska, K., Sikora, J., Dulebova, L., (2017), Properties of moldings prepared from ldpe-pumpkin seed hulls blend. Advances in Science and Technology Research Journal, 11(4), pp. 318-325.

[2] Sikora, J.W., Gajdoš, I., Puszka, A., (2019), Polyethylene-matrix composites with halloysite nanotubes with enhanced physical/thermal properties, Polymers, 11(5), 787.

[3] Sikora, J.W., Majewski, Ł., Puszka, A., Modern Biodegradable Plastics - Processing and Properties: Part I. Materials 2020, vol. 13, nr 8, s. 1-22.

[4] Jachowicz, T., Sikora, J., Dulebova L., (2017), Investigating effects of prodegradant content on selected properties of polymer composite materials, Environmental Engineering and Management Journal 16(12), pp. 2879-2886.

[5] Sikora, J.W., (2014), Feeding an extruder of a modified feed zone design with poly(vinyl chloride) pellets of variable geometric properties, International Polymer Processing, 29(3), pp. 412-418.

[6] Sikora, J., Samujło, B., (2013), Impact of feed opening width and position on pvc extrusion process effectiveness, International Polymer Processing, 28(3), pp. 291-299.

[7] Sasimowski, E., Sikora, J., Królikowski, B., (2014), Effectiveness of polyethylene extrusion in a single-screw grooved feed extruder, Polimery, 59(6), pp. 505-510.

[8] Dębski, H., Ferdynus, M., Sikora, J.W., (2020), A concept for a novel polymer extruder. Part I., Facta Universitatis-Series Mechanical Engineering, 17(1), pp. 1-15.

[9] Sikora, R., Sasimowski, E., Sikora, J.W., (2011), Dihelicoidal extrusion. Principles and processing, Polimery, 56(7-8), pp. 591-596.

[10] Sasimowski, E., (2011), Studies in the effectiveness of a new generation extruder. Part I. The influence of the location of the rotating sleeve of the barrel in the plasticizing system, Polimery, 56(5), pp. 390-396.

[11] Sasimowski, E., (2012), Studies in the effectiveness of a new generation extruder. Part III. Co-operation of the rotational sleeve with the grooved zone of barrel, Polimery, 57(10), pp. 747-754.

[12] Marinković, D., Rama, G., Zehn, M., (2019), Abaqus implementation of a corotational piezoelectric 3-node shell element with drilling degree of freedom, Facta Universitatis - Series Mechanical Engineering, 17(2), pp. 269-283.

[13] Sengupta, J., Cockcroft, S.L., Maijer, D.M., Larouche, A., (2005), Quantification of temperature, stress, and strain fields during the start-up phase of a direct chill casting process by using a 3D fully coupled thermal and stress model for AA5182 ingots, Materials Science and Engineering: A, 397(1-2), pp. 157-177.

[14] Krstić, V., Milčić, D., Milčić, A., (2018), A thermal analysis of the threaded spindle bearing assembly in numerically controlled machine tools, Facta Universitatis-Series: Mechanical Engineering, 16(2), pp. 261-272.

[15] Bakari, H.R., Adegoke, T.M., Yahya, A.M., (2016), Application of newton-raphson method to non-linear models. International Journal of Mathematics and Statistics Studies, 4(4), pp. 21-31.

[16] Horiguchi, S., (2016), The Formulas to compare the convergences of newton's method and the extended Newton's method (Tsuchikura-Horiguchi Method) and the numerical calculations. Applied Mathematics 7(1), pp. 40-60.

[17] Justus Benad, (2019), Numerical methods for the simulation of deformations and stresses in turbine blade fir-tree connections, Facta Universitatis-Series: Mechanical Engineering, 17(1), pp. 1-15.

Acknowledgements